



Effect of Tie Beam Breadth on the Behavior of Isolated Footings during Earthquakes

Elsamny, M. K.¹, Ezz-Eldeen, H. A.¹, Elbatal, S. A.¹ and Elmalahy, A. S.²

¹Civil Engineering, Faculty of Engineering, Al-Azhar University, Cairo, Egypt

²The Arab Contractors, Sinai Branch, Ismailia, Egypt

me@elmalahyas.xyz

Abstract: Generally, designers of low-rise buildings that resting on shallow foundations consider the fixed base condition results and ignore the soil-structure interaction lead to unsafe design due to seismic load. In this paper an investigation of tie beam dimensions effect on isolated footings connected with tie beams under dynamic load (earthquake using Response Spectrum based on ECP 201-2008). A finite element analysis PLAXIS 3D 2013 has been used to analysis the model. The investigated program consists of earthquake wave applied on the superstructure that resting on isolated footings connected with tie beams with variable dimensions. It was found that; increasing of tie beam breadth decreases the vertical displacement in Z-direction about (10 to 25) % in static load and about (10 to 20) % in dynamic load. However, the horizontal displacement in both Y and X directions decreases about (30 to 50) % in static load and about (15 to 30) % in dynamic load. The contact pressure decreases by (27) % by increasing tie beam breadth in case of static load decrease but in dynamic load about (15)%. In addition, the bending moment along axis decrease by increasing tie beam breadth by (20) % in static and dynamic load. In addition to that the vertical displacement in Z-direction decreases with increasing the internal friction angle for sandy soil up to $\phi \leq 36^\circ$ and in cases of $\phi > 36^\circ$ no significant change in the vertical displacement in Z-direction as well as no significant change in total normal stress (contact pressure) distributions shape but the value of total normal stress decreases by increasing angle of internal friction. The value of total normal stress decreases by increasing tie beam breadth.

[Elsamny, M. K., Ezz-Eldeen, H. A., Elbatal, S. A. and Elmalahy, A. S. **Effect of Tie Beam Breadth on the Behavior of Isolated Footings during Earthquakes.** *J Am Sci* 2020;16(4):1-16]. ISSN 1545-1003 (print); ISSN 2375-7264 (online). <http://www.jofamericanscience.org>. 1. doi:[10.7537/marsjas160420.01](https://doi.org/10.7537/marsjas160420.01).

Key words: Tie beam, Displacements, contact pressure, Shear stresses, Bending moment, PLAXIS, Finite Element, Dynamic load, Earthquakes.

1. Introduction

Analysis of foundation that subjected to dynamic load has become a substantial problem in civil engineering. Several major earthquakes that caused dangerous damages to structures have brought a lot of attention to how foundations behave under dynamic loading. During earthquakes stresses distribution below the footings become non-uniform causing unequal settlement. Tie beams are used to connect isolated footings, in two directions. However, the system of footings and tie beams is considered as rigid and should be treated as one entity, As the tie beams play an important role for redistribution of column loads between footings through it.

Khalil, A. A. (2000)^[1] studied the analysis of soil interaction for wall on a strip footing or two isolated footings connected with tie beam. The used finite element method was to study the problem. 3D solid elements were used to calculate the beam, columns and footings as well as soil was represented by Winkler model. A parametric study contained soil nonuniformity, soil stiffness, beam depth and the level of tie beam relative to the footing was performed. The

effects of these parameters on the load distribution between the footings and the tie beams, the stresses and the relative settlement in the tie beam were studied.

Al-Omari, R. R. and Al-Ebadi, L. H. (2008)^[2] investigated the tie beams effect on settlement, bending moments and shear force in the foundation. 3D finite analyses performed. The detailed results indicated that the tie beams reduce the total and differential settlements of footings.

Almassmoum A. A. (2009)^[3] presented the effect of tie beams connected with middle footing and strap beams connected with eccentric footing on the contact pressure. The maximum percentage ratio of differential displacement to length of tie beam, the ratio of column load carried by tie beams were investigated.

El-Samny, M. K. et. al. (2010)^[4] studied the Young's modulus "Es" of cohesion less soil at surface under footings with and without surcharge in field for graded sand samples. The tests have been done in field by using plate load test.

The settlement has been measured under various stress levels at the surface along the center line of the plate and the edge of the plate. Also, under different applied stresses the settlement has been measured.

Mahdy, M. (2011) ^[5] measured the shape of displacement of soil under two rigid plates connected with tie. The settlement has been measured at surface and at various depths ($B/2$, B and $1.50 B$ where B = width of plates) with and without surcharge. It was concluded that the settlement of cohesion less soil for square plate with dimensions (305 x 305) is less than the settlement of rectangular plate with dimensions (305 x 610) mm. However, settlement increases by increasing tie beam length of both square and rectangular footing. Almasri, A. H. and Taqieddin, Z. N. (2012) studied the important of tie beam to improve to resist the structural settlement using finite analysis of three-dimensional structural models. Although, investigated the behavior of tie beam under earth quake loading to improve the performance of footings system. It was found that tie beams in both dynamic load and static load reduced differential settlement.

Elsamny, M. K., et al (2012) ^[6] investigated the effect of tie beam length on settlement of soil is the different parameters. A theoretical formulii has been investigated to calculate the settlement for the rectangular and the square footings with tie beam with the effect of surcharge.

Farouk, M. (2012) ^[7] determined the settlement under footings connected with tie beams. An empirical formula was calculated to investigate the displacement for two footing connected with tie beam. PLAXIS version 7.2 was used to determine the displacement field of soil as well as the settlement under footings.

El-sedeek, M. B. (2013) ^[8] studied the tie beam width effect as well as length on overlap- stress and settlement of foundation. In case of tie beam, an equation is studied to calculate the overlap stress zone. Also, it was concluded that increasing the tie beam length leads to increasing settlement. In case of tie beam, the width of overlap stress zone founded to be equal to (1.6-1.75) B . The settlement of footings decreases with increasing tie beam width. Also, it is found that the settlement with the effect of overlap stress zone increases with increasing the tie beam length.

Basha, A. M. and Salama, M. I. (2017) ^[9] analyzed the effect of tie beams on differential settlement. 3-D analysis of the tie beams connected to isolated footings system by the finite method was conducted. The analytical result founded that increasing width of tie beam leads to increasing bending moments carried by the tie beam.

Elsamny, M. K., et al. (2017) ^[10] studied the behavior of two isolated footings connected with tie

beam with different dimensions. one of this footing has fixed dimension. The second footing has different length. And the thickness was variable ($t=0.3B$, $0.4B$, $0.5B$ and $0.6B$) where ($B=1.0m$) the footing width. The tie beam length was variable ($L_{tie}=0.5B$, $1.0B$, $1.5B$ and $2.0B$). The height of the tie beams between footing was ($h=1.0t$, $1.5t$, $2.0t$ and $2.5t$) and the width of tie beam was fixed ($b=0.25m$). Also, studied the effect of depth of footing where ($df=0.0B$, $0.5B$, $1.0B$ and $1.5B$). In addition, the angle of internal friction in sandy soil was taken ($\phi=30^\circ$, 35° , 40° and 45°). However, cohesion for clayey soil was taken as ($c=10$, 15 , 20 and 25) kN/m^2 . It was investigated that increasing tie beam length leads to increasing the vertical and horizontal displacement in both directions. Also, increasing the angle of internal friction and cohesion leads to decreasing the vertical and horizontal displacement in both directions. The vertical and horizontal displacement decreased with increasing the height of tie beam.

Elsamny, M. K. et. al. (2018) ^[11] investigated the tie beam thickness and width effect on footings under eccentric loading on vertical, horizontal displacement and contact pressure, moment and shear.

It was found that in eccentric loading, increasing the thickness and width of tie beams leads to decreasing the vertical displacement and horizontal displacement by about (20 to 40) %. The displacement almost uniform along axis. Differential settlement decreases by increasing the thickness and width of tie beam. Also, it was found that increasing width of tie beam and tie beam thickness leads to decreasing the values of the total normal stress (contact pressure) by about (30 to 40) %. It was also found the bending moment as well as shear force values decrease with increasing the thickness and width of tie beams by about (30 to 40) %.

Vincenzo P., et al. (2019) ^[12] investigated the effect of tie beams connecting eccentrically loaded footings. It was shown that in some design situations, which were relatively frequent in high seismicity regions, the tie beams can furnish a significant contribution to reduce the bending moment transferred to the ground.

However; needing to evaluate the effect of tie beam dimensions on the behavior of isolated footings that connected with tie beams especially during earthquakes. This paper presents fully three-dimension model to simulate the foundation which supported superstructure and rested on soil media as well as exposed to dynamic load using Response Spectrum based on ECP 201-2008.

The objectives of the presented study are to determine the effect of tie beam breadth on the behavior of isolated footings connected with tie beams as follows:

i. Study the effect of tie beam breadth on the vertical displacement in Z-direction in case of dynamic and static load.

ii. Study the effect of tie beam breadth on the horizontal displacement in both X and Y directions in case of dynamic and static load.

iii. Study the effect of tie beam breadth on the contact pressure and vertical shear stress in case of dynamic and static load.

iv. Study the effect of tie beam breadth on the bending moment in case of dynamic and static load.

2. Analytical Analysis by Finite Element Model

A scientific finite element package "PLAXIS - 3D version 2013" was used to simulate the proposed numerical model.

2.1. Proposed Model

In the present study, a theoretical analysis has been done for superstructure model (B×L) where; B in X-direction as shown in figure (1) and its properties listed in table (1). The superstructure resting on system of twenty isolated footings (5×4) as shown in figure (1) and its dimensions listed in table (2) these footings connected with tie beams with variable cross

sections and length listed in table (3) and shown in figure (2). A finite element package of the PLAXIS version 2013 has been used to simulate the chosen model. Mohr-Coulomb model has been used to represent the soil behavior. The material properties for soil which has been used in the finite element model are shown in table (4). All of the above assumptions have used with constant depth of footing ($D_F = 0.00$ m).

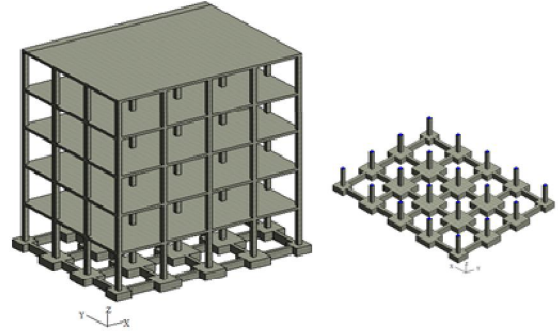


Figure [1] 3D Model for the Proposed Structure and the System of footings with tie beams

Table [1] Superstructure data

Columns	0.35 x 0.35 m
Slab	0.2 m thick
Floor height	3 m
Type of support	Pinned
Floor finish	1.5 kN/m ²
Live load	2.0 kN/m ²
Density of concrete	25 kN/m ³
Density of brick wall	18 kN/m ³

Table [2] Dimensions of isolated footings

Footings	No. of footings	Dimensions (m)		
		B	L	D
		Width	length	thickness
Corner	4	1.35	1.35	0.6
Edge	10	1.85	1.85	0.6
Central	6	2.45	2.45	0.6

2.2. Modeling of the Used Elements

2.2.1. Model of Soil

Boreholes: Layers of soil are determined by means of boreholes. In the geometry multiple boreholes placed to determine an inclined ground surface or a non-horizontal soil stratigraphy. Automatically PLAXIS (3D) interpolates ground

surface and layer in between the boreholes. Alternatively, a TIN surface can be assigned to a borehole to characterize the ground surface.

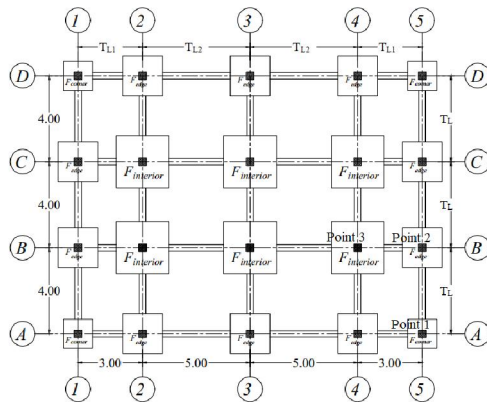
Mohr-Coulomb model was used to modeling the soil, the proposed models were investigated under constant type of soil (sandy soil with different friction angle).

Table [3] Investigated tie beams cross sections and length

No.	Tie beam dimensions		
	Breadth (m)	Height (m)	Length (m)
1	0.30	0.60	$L_{T1} = 3.00$ m $L_{T2} = 5.00$ m
2		0.75	
3		0.90	
4		1.05	

Table [4] The material properties for the soil

Parameters	Name	sandy soil	unit
Material model	Model	Moher-coulomb	-
Material behavior	Type	Drained	-
unsaturated soil weight	γ_{unsat}	17.5	KN/m ³
saturated soil weight	γ_{sat}	20	KN/m ³
Poisson ratio	ν	0.3	-
Cohesion	c	-	KN/m ²
Friction angle	ϕ	30,35,40,45	°
Dilatancy	Ψ	0,5,10,15	°

**Figure [2]** Plan of System of footings with tie beams

2.2.2. Model of Structure Element

2.2.2.1. Model of Footings and Floors

Footings and floors elements are different from the 6-node triangles in the sense that they have six degrees of freedom per node instead of three, i.e. three translational d.o.f.s (u_x , u_y , u_z) and three rotational d.o.f.s (ϕ_x , ϕ_y , ϕ_z). These elements are numerically integrated using 2×3 point Gaussian integration.

Plates: These special features can be used to model thin two-dimensional structures in the ground with a significant flexural rigidity (bending stiffness).

The basic geometry parameters in plates include the thickness d , and the unit weight of the floor material g . Distinct stiffnesses can be specified for the different floor directions. As an alternative for the linear elastic properties, non-linear elastic properties may be specified by means of (M-k) and (N-e) diagrams. Structural forces are evaluated from the stresses at the stress points (see Scientific Manual) and extrapolated to the element nodes. These forces

can be viewed graphically and tabulated in the Output program. contrast to walls, there are no interface elements generated along floors.

2.2.2.2. Model of Beams and Columns

The 3-node beam elements are used at the edges of other structural elements. Beam elements are slightly different from 3-nodeline element in the sense that they have six degrees of freedom per node instead of three, i.e. three translational d.o.f.s (u_x , u_y , u_z) and three rotational d.o.f.s (ϕ_x , ϕ_y , ϕ_z). These elements are numerically integrated using 4-point Gaussian integration. The element provides a quadratic interpolation of the longitudinal displacements and a fifth-order interpolation of transverse displacements. For beam elements, there is one local coordinate (ξ).

Beams are structural objects used to model slender (one-dimensional) structures in the ground with a significant flexural rigidity (bending stiffness) and an axial stiffness. coincide with the active work plane.

The basic geometry parameters include the cross-section area A , and the unit weight of the beam material. Distinct moments of inertia can be specified for bending in horizontal and vertical direction. As an alternative for the linear elastic properties, non-linear elastic properties may be specified by means of (M-k) and (N-e) diagrams. Structural forces are evaluated from the stresses at the stress points (see Scientific manual) and extrapolated to the element nodes.

2.2.3.3D Dynamics Module

The PLAXIS Dynamics module is an add-on module. This module may be used to analyses vibrations in the soil and their influence on nearby structures. Excess pore pressures can be analyzed. Liquefaction.

3. Analytical Analysis Results

Figure (3) show deformed mesh of soil and the structure where; tie beam dimensions are breadth ($T_B = 0.30$ m), height ($T_H = 0.60$ m), length ($T_{L1} = 3.00$ & $T_{L2} = 5.00$ m), depth of footing ($D_F = 0.00$ m) and internal friction angle ($\phi = 30^\circ$).

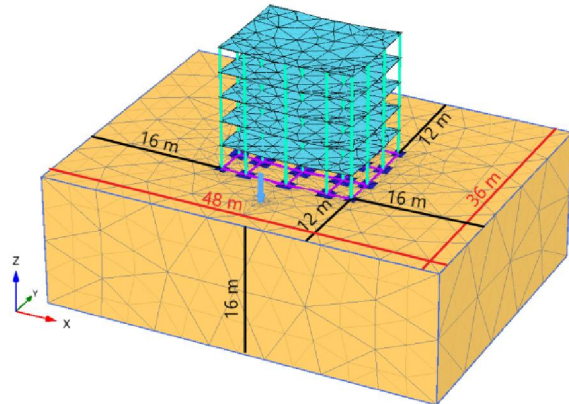


Figure [3] Deformed mesh for the model where; $T_B = 0.30$ m, $T_H = 0.60$ m, length $T_{L1} = 3.00$ & $T_{L2} = 5.00$ m, $D_F = 0.00$ m and $\phi = 30^\circ$

Figures (4) and (5) Vertical displacement in Z-direction underneath footings as shading where; $T_B = 0.30$ m, $T_H = 0.60$ m, $T_{L1} = 3.00$ & $T_{L2} = 5.00$ m, $D_F = 0.00$ m and $\phi = 30^\circ$ in case of dynamic and static load.

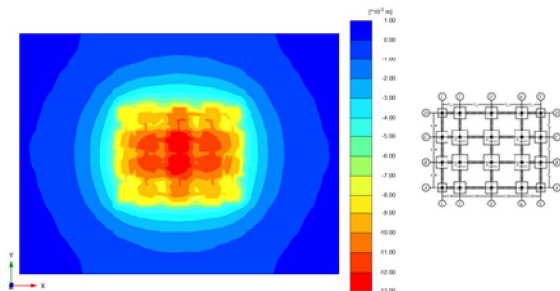


Figure [4] Vertical displacement in Z-direction underneath footings where; $T_B = 0.30$ m, $T_H = 0.60$ m, $T_{L1} = 3.00$ & $T_{L2} = 5.00$ m, $D_F = 0.00$ m and $\phi = 30^\circ$ in case of static load

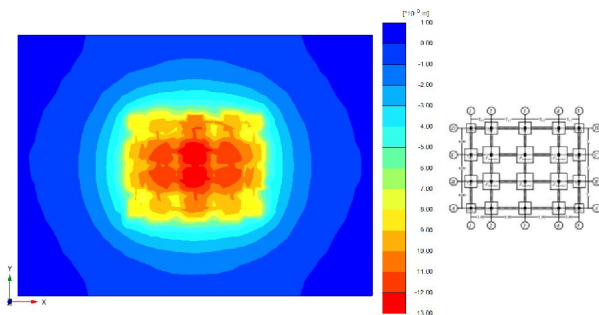


Figure 5 Vertical displacement in Z-direction underneath footings where; $T_B = 0.30$ m, $T_H = 0.60$ m, $T_{L1} = 3.00$ & $T_{L2} = 5.00$ m, $D_F = 0.00$ m and $\phi = 30^\circ$ in case of dynamic load

Figures (6) and (7) Horizontal displacement in X-direction underneath footings as shading where; $T_B = 0.30$ m, $T_H = 0.60$ m, $T_{L1} = 3.00$ & $T_{L2} = 5.00$ m, $D_F = 0.00$ m and $\phi = 30^\circ$ in case of dynamic and static load.

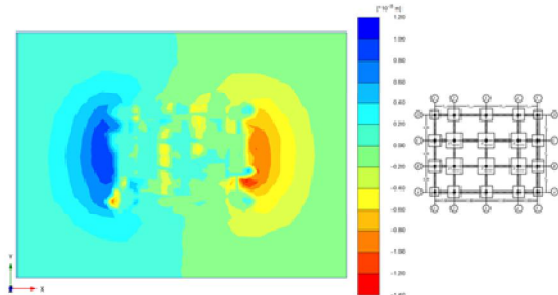


Figure [6] Horizontal displacement in X-direction underneath footings where; $T_B = 0.30$ m, $T_H = 0.60$ m, $T_{L1} = 3.00$ & $T_{L2} = 5.00$ m, $D_F = 0.00$ m and $\phi = 30^\circ$ in case of static load

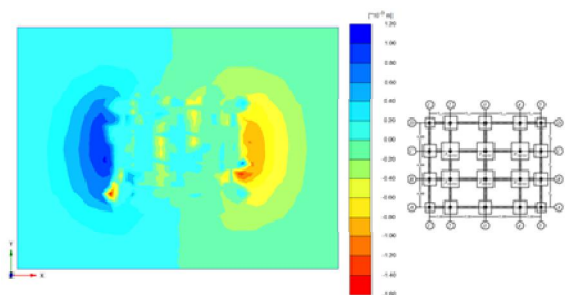


Figure [7] Horizontal displacement in X-direction underneath footings where; $T_B = 0.30$ m, $T_H = 0.60$ m, $T_{L1} = 3.00$ & $T_{L2} = 5.00$ m, $D_F = 0.00$ m and $\phi = 30^\circ$ in case of dynamic load

Figures (8) and (9) Horizontal displacement in Y-direction underneath footings as shading where; $T_B = 0.30$ m, $T_H = 0.60$ m, $T_{L1} = 3.00$ & $T_{L2} = 5.00$ m, $D_F = 0.00$ m and $\phi = 30^\circ$ in case of dynamic and static load.

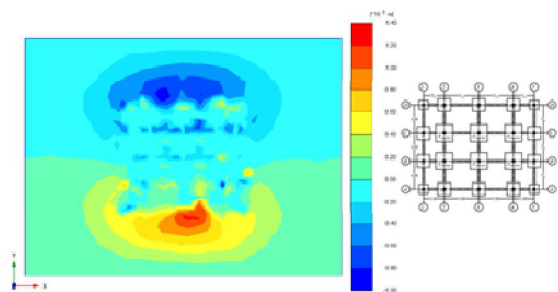


Figure [8] Horizontal displacement in Y-direction underneath footings where; $T_B = 0.30$ m, $T_H = 0.60$ m, $T_{L1} = 3.00$ & $T_{L2} = 5.00$ m, $D_F = 0.00$ m and $\phi = 30^\circ$ in case of static load

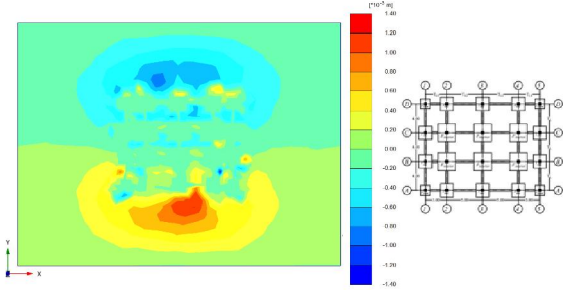


Figure [9] Horizontal displacement in Y-direction underneath footings where; $T_B = 0.30$ m, $T_H = 0.60$ m, $T_{L1} = 3.00$ & $T_{L2} = 5.00$ m, $D_F = 0.00$ m and $\phi = 30^\circ$ in case of dynamic load

Figures (10) and (11) Vertical displacement in Z-direction along axis (A-A) as shading where; $T_B = 0.30$ m, $T_H = 0.60$ m, $T_{L1} = 3.00$ & $T_{L2} = 5.00$ m, $D_F = 0.00$ m and $\phi = 30^\circ$ in case of dynamic and static load.

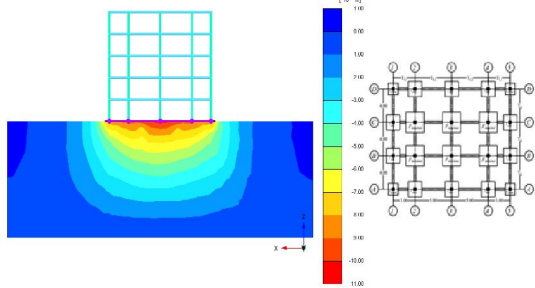


Figure [10] Vertical displacement in Z-direction along axis (A-A) where; $T_B = 0.30$ m, $T_H = 0.60$ m, $T_{L1} = 3.00$ & $T_{L2} = 5.00$ m, $D_F = 0.00$ m and $\phi = 30^\circ$ in case of static load

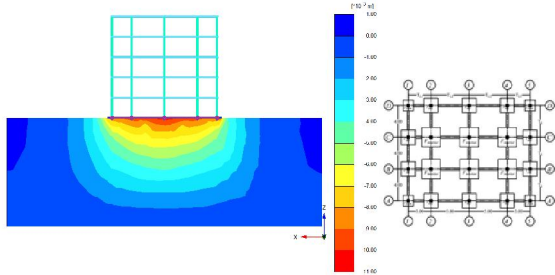


Figure [11] Vertical displacement in Z-direction along axis (A-A) where; $T_B = 0.30$ m, $T_H = 0.60$ m, $T_{L1} = 3.00$ & $T_{L2} = 5.00$ m, $D_F = 0.00$ m and $\phi = 30^\circ$ in case of dynamic load

Figures (12) and (13) Horizontal displacement in X-direction along axis (A-A) as shading where; $T_B = 0.30$ m, $T_H = 0.60$ m, $T_{L1} = 3.00$ & $T_{L2} = 5.00$ m, $D_F = 0.00$ m and $\phi = 30^\circ$ in case of dynamic and static load.

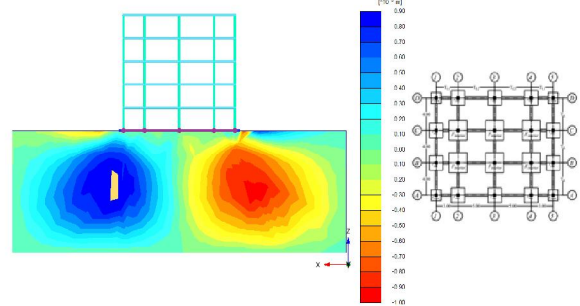


Figure [12] Horizontal displacement in X-direction along axis (A-A) where; $T_B = 0.30$ m, $T_H = 0.60$ m, $T_{L1} = 3.00$ & $T_{L2} = 5.00$ m, $D_F = 0.00$ m and $\phi = 30^\circ$ in case of static load

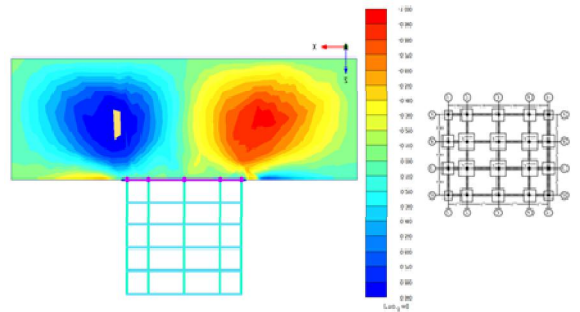


Figure [13] Horizontal displacement in X-direction along axis (A-A) where; $T_B = 0.30$ m, $T_H = 0.60$ m, $T_{L1} = 3.00$ & $T_{L2} = 5.00$ m, $D_F = 0.00$ m and $\phi = 30^\circ$ in case of dynamic load

Figures (14) and (15) Horizontal displacement in Y-direction along axis (A-A) as shading where; $T_B = 0.30$ m, $T_H = 0.60$ m, $T_{L1} = 3.00$ & $T_{L2} = 5.00$ m, $D_F = 0.00$ m and $\phi = 30^\circ$ in case of dynamic and static load.

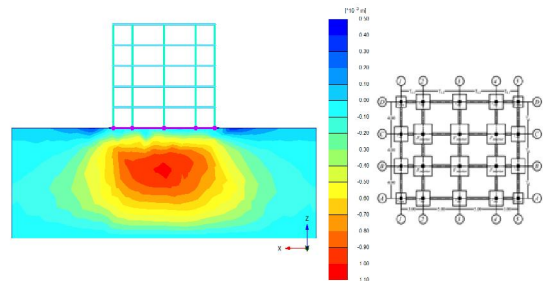


Figure [14] Horizontal displacement in Y-direction along axis (A-A) where; $T_B = 0.30$ m, $T_H = 0.60$ m, $T_{L1} = 3.00$ & $T_{L2} = 5.00$ m, $D_F = 0.00$ m and $\phi = 30^\circ$ in case of static load

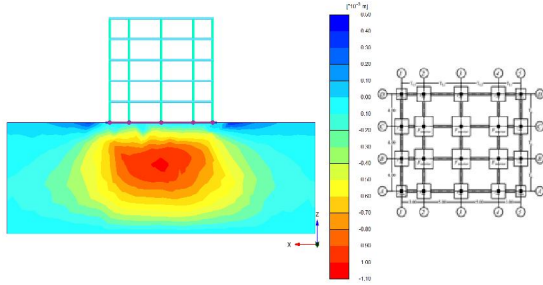


Figure [15] Horizontal displacement in Y-direction along axis (A-A) where; $T_B = 0.30$ m, $T_H = 0.60$ m, $T_{L1} = 3.00$ & $T_{L2} = 5.00$ m, $D_F = 0.00$ m and $\phi = 30^0$ in case of dynamic load

Figures (16) and (17) Contact pressure underneath footings as shading where; $T_B = 0.30$ m, $T_H = 0.60$ m, $T_{L1} = 3.00$ & $T_{L2} = 5.00$ m, $D_F = 0.00$ m and $\phi = 30^0$ in case of dynamic and static load.

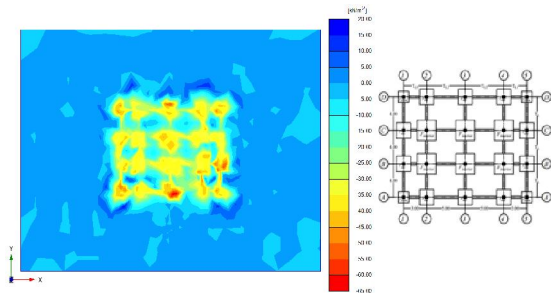


Figure [16] Contact pressure underneath footings where; $T_B = 0.30$ m, $T_H = 0.60$ m, $T_{L1} = 3.00$ & $T_{L2} = 5.00$ m, $D_F = 0.00$ m and $\phi = 30^0$ in case of static load

Figures (18) and (19) Contact pressure along axis (A-A) as shading where; $T_B = 0.30$ m, $T_H = 0.60$ m, $T_{L1} = 3.00$ & $T_{L2} = 5.00$ m, $D_F = 0.00$ m and $\phi = 30^0$ in case of dynamic and static load.

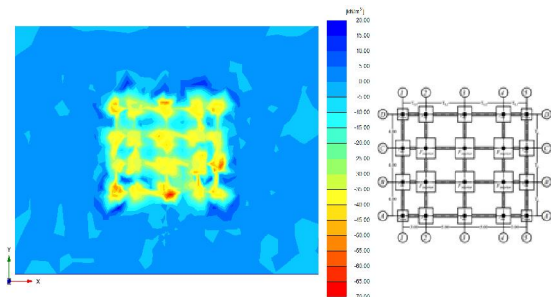


Figure [17] Contact pressure underneath footings where; $T_B = 0.30$ m, $T_H = 0.60$ m, $T_{L1} = 3.00$ & $T_{L2} = 5.00$ m, $D_F = 0.00$ m and $\phi = 30^0$ in case of dynamic load

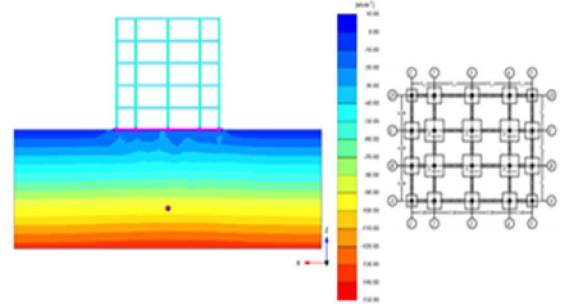


Figure [18] Contact pressure along axis (A-A) where; $T_B = 0.30$ m, $T_H = 0.60$ m, $T_{L1} = 3.00$ & $T_{L2} = 5.00$ m, $D_F = 0.00$ m and $\phi = 30^0$ in case of static load

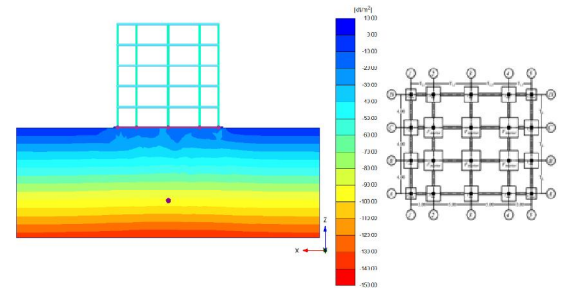


Figure [19] Contact pressure along axis (A-A) where; $T_B = 0.30$ m, $T_H = 0.60$ m, $T_{L1} = 3.00$ & $T_{L2} = 5.00$ m, $D_F = 0.00$ m and $\phi = 30^0$ in case of dynamic load

Figures (20) and (21) Vertical shear stress underneath footings as shading where; $T_B = 0.30$ m, $T_H = 0.60$ m, $T_{L1} = 3.00$ & $T_{L2} = 5.00$ m, $D_F = 0.00$ m and $\phi = 30^0$ in case of dynamic and static load.

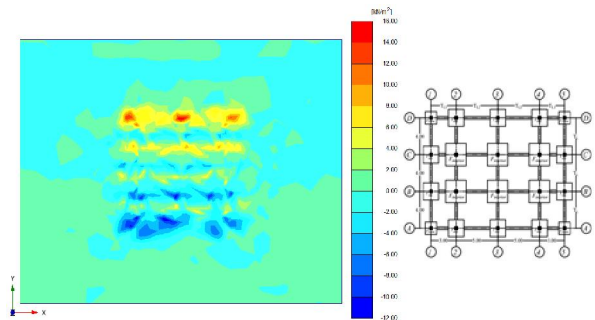


Figure [20] Vertical shear stress underneath footings where; $T_B = 0.30$ m, $T_H = 0.60$ m, $T_{L1} = 3.00$ & $T_{L2} = 5.00$ m, $D_F = 0.00$ m and $\phi = 30^0$ in case of static load

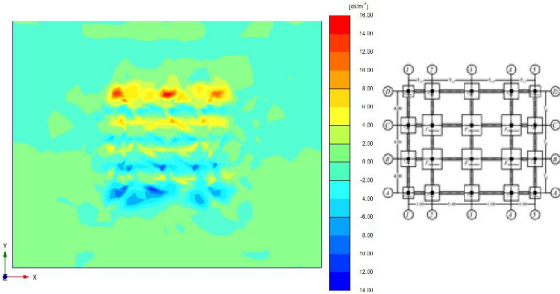


Figure [21] Vertical shear stress underneath footings where; $T_B = 0.30$ m, $T_H = 0.60$ m, $T_{L1} = 3.00$ & $T_{L2} = 5.00$ m, $D_F = 0.00$ m and $\phi = 30^0$ in case of dynamic load

Figures (22) and (23) Vertical shear stress along axis (A-A) as shading where; $T_B = 0.30$ m, $T_H = 0.60$ m, $T_{L1} = 3.00$ & $T_{L2} = 5.00$ m, $D_F = 0.00$ m and $\phi = 30^0$ in case of dynamic and static load.

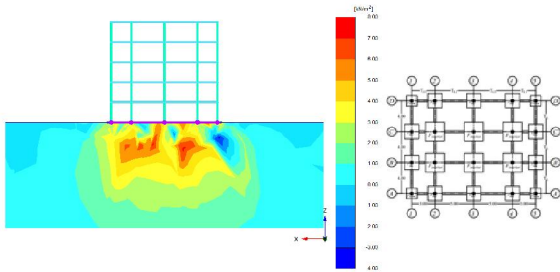


Figure [22] Vertical shear stress along axis (A-A) where; $T_B = 0.30$ m, $T_H = 0.60$ m, $T_{L1} = 3.00$ & $T_{L2} = 5.00$ m, $D_F = 0.00$ m and $\phi = 30^0$ in case of static load

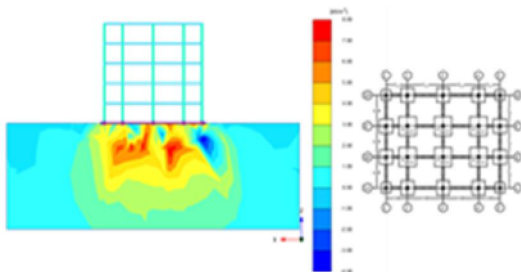


Figure [23] Vertical shear stress along axis (A-A) where; $T_B = 0.30$ m, $T_H = 0.60$ m, $T_{L1} = 3.00$ & $T_{L2} = 5.00$ m, $D_F = 0.00$ m and $\phi = 30^0$ in case of dynamic load

4. Analysis of Results

4.1. Effect of Tie Beam Breadth (T_b)

Figures (24) and (25) show relationship between vertical displacement in Z-direction and distance along axis (A-A) where; $D_F = 0.00$ m, $\phi = 30^0$, $T_H = 0.60$ m, $T_{L1} = 3.00$ m, $T_{L2} = 5.00$ m and different tie beam breadth in case of static and dynamic load respectively.

From this figure; it can be shown the vertical displacement decreases by increasing tie beam breadth about (10 to 25) % in case of static load as well as about (10 to 20) % in case of dynamic load.

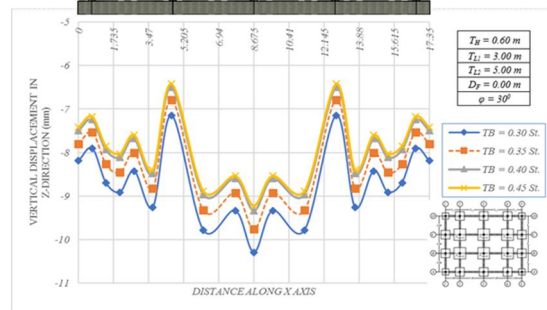


Figure [24] Relationship between vertical displacement in Z-direction and distance along axis (A-A) in case of static load with different tie beam breadth where; $T_H = 0.60$ m, $T_{L1} = 3.00$ m, $T_{L2} = 5.00$ m, $D_F = 0.00$ and $\phi = 30^0$

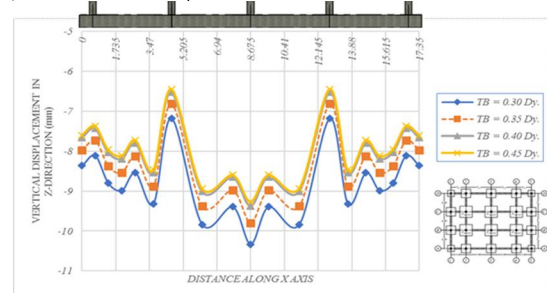


Figure [25] Relationship between vertical displacement in Z-direction and distance along axis (A-A) in case of dynamic load with different tie beam breadth where; $T_H = 0.60$ m, $T_{L1} = 3.00$ m, $T_{L2} = 5.00$ m, $D_F = 0.00$ and $\phi = 30^0$

Figure (26) show comparison between vertical displacement in Z-direction in case of static load and dynamic load at different tie beam breadth where; $D_F = 0.00$ m, $\phi = 30^0$, $T_H = 0.60$ m, $T_{L1} = 3.00$ m, $T_{L2} = 5.00$ m.

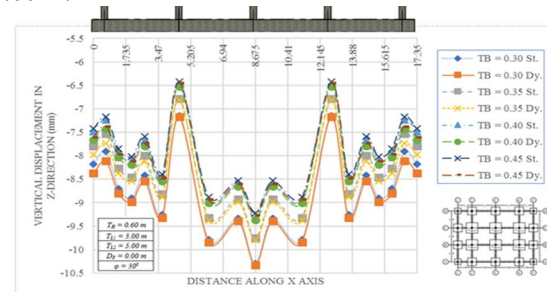


Figure [26] Comparison between vertical displacement in Z-direction along axis (A-A) in case of static and dynamic load with different tie beam breadth where; $T_H = 0.60$ m, $T_{L1} = 3.00$ m, $T_{L2} = 5.00$ m, $D_F = 0.00$ and $\phi = 30^0$

Figures (27) and (28) show relationship between horizontal displacement in X-direction and distance along axis (A-A) where; $D_F = 0.00$ m, $\phi = 30^\circ$, $T_H = 0.60$ m, $T_{L1} = 3.00$ m, $T_{L2} = 5.00$ m and different tie beam breadth in case of static and dynamic load respectively.

From this figure; it can be shown the vertical displacement decreases by increasing tie beam breadth about (30 to 50) % in case of static load as well as about (15 to 30) % in case of dynamic load.

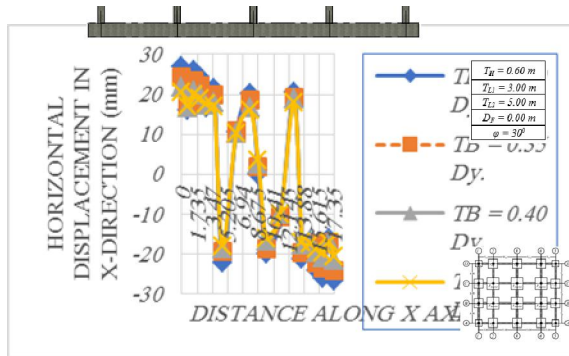


Figure [27] Relationship between horizontal displacement in X-direction and distance along axis (A-A) in case of static load with different tie beam breadth where; $T_H = 0.60$ m, $T_{L1} = 3.00$ m, $T_{L2} = 5.00$ m, $D_F = 0.00$ and $\phi = 30^\circ$

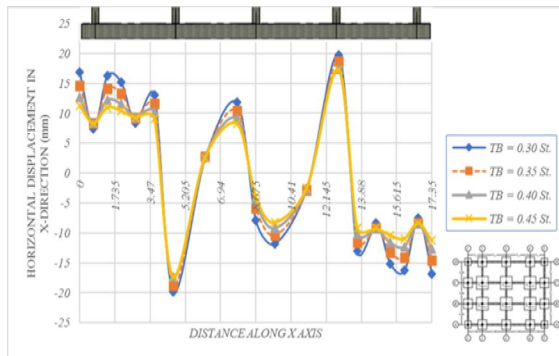


Figure [28] Relationship between horizontal displacement in X-direction and distance along axis (A-A) in case of dynamic load with different tie beam breadth where; $T_H = 0.60$ m, $T_{L1} = 3.00$ m, $T_{L2} = 5.00$ m, $D_F = 0.00$ and $\phi = 30^\circ$

Figure (29) show comparison between horizontal displacement in X-direction in case of static load and dynamic load at different tie beam breadth where; $D_F = 0.00$ m, $\phi = 30^\circ$, $T_H = 0.60$ m, $T_{L1} = 3.00$ m, $T_{L2} = 5.00$ m.

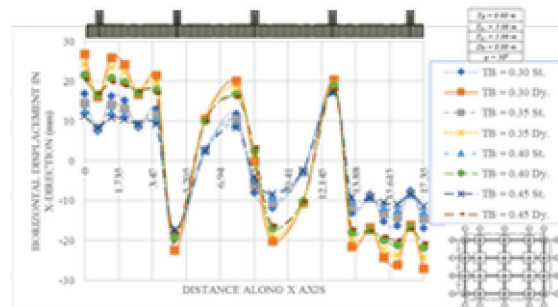


Figure [29] Comparison between horizontal displacement in X-direction along axis (A-A) in case of static and dynamic load with different tie beam breadth where; $T_H = 0.60$ m, $T_{L1} = 3.00$ m, $T_{L2} = 5.00$ m, $D_F = 0.00$ and $\phi = 30^\circ$

Figures (30) and (31) show relationship between horizontal displacement in Y-direction and distance along axis (A-A) where; $D_F = 0.00$ m, $\phi = 30^\circ$, $T_H = 0.60$ m, $T_{L1} = 3.00$ m, $T_{L2} = 5.00$ m and different tie beam breadth in case of static and dynamic load respectively. From this figure; it can be shown the vertical displacement decreases by increasing tie beam breadth about (30 to 50) % in case of static load as well as about (15 to 30) % in case of dynamic load.

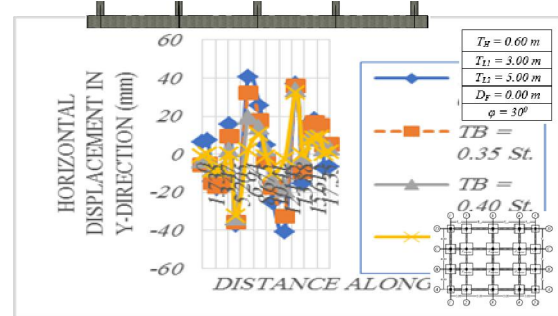


Figure [30] Relationship between horizontal displacement in Y-direction and distance along axis (A-A) in case of static load with different tie beam breadth where; $T_H = 0.60$ m, $T_{L1} = 3.00$ m, $T_{L2} = 5.00$ m, $D_F = 0.00$ and $\phi = 30^\circ$

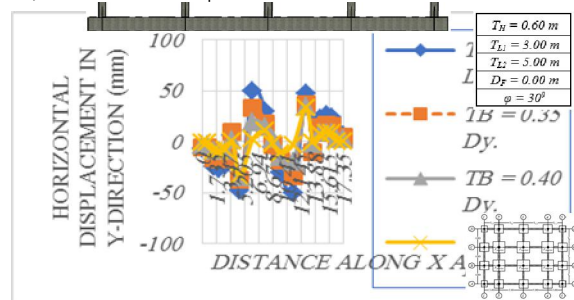


Figure [31] Relationship between horizontal displacement in Y-direction and distance along axis (A-A) in case of dynamic load with different tie beam breadth where; $T_H = 0.60$ m, $T_{L1} = 3.00$ m, $T_{L2} = 5.00$ m, $D_F = 0.00$ and $\phi = 30^\circ$

Figure (32) show comparison between horizontal displacement in Y-direction in case of static load and dynamic load at different tie beam breadth where; $D_F = 0.00$ m, $\phi = 30^\circ$, $T_H = 0.60$ m, $T_{L1} = 3.00$ m, $T_{L2} = 5.00$ m.

Figures (33) and (34) show relationship between contact pressure and distance along axis (A-A) where; $D_F = 0.00$ m, $\phi = 30^\circ$, $T_H = 0.60$ m, $T_{L1} = 3.00$ m, $T_{L2} = 5.00$ m and different tie beam breadth in case of static and dynamic load respectively. From this figure; it can be shown the vertical displacement decreases by increasing tie beam breadth about (27) % in case of static load as well as about (15) % in case of dynamic load.

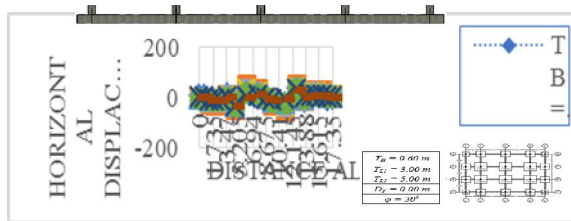


Figure [32] Comparison between horizontal displacement in Y-direction along axis (A-A) in case of static and dynamic load with different tie beam breadth where; $T_H = 0.60$ m, $T_{L1} = 3.00$ m, $T_{L2} = 5.00$ m, $D_F = 0.00$ and $\phi = 30^\circ$

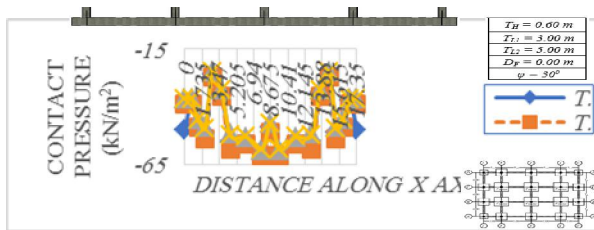


Figure [33] Relationship between contact pressure and distance along axis (A-A) in case of static load with different tie beam breadth where; $T_H = 0.60$ m, $T_{L1} = 3.00$ m, $T_{L2} = 5.00$ m, $D_F = 0.00$ and $\phi = 30^\circ$

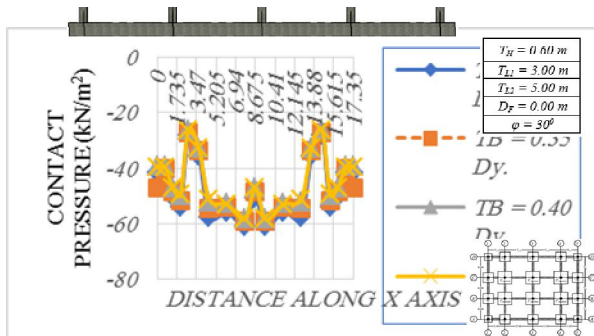


Figure [34] Relationship between contact pressure and distance along axis (A-A) in case of dynamic load with different tie beam breadth where; $T_H = 0.60$ m, $T_{L1} = 3.00$ m, $T_{L2} = 5.00$ m, $D_F = 0.00$ and $\phi = 30^\circ$

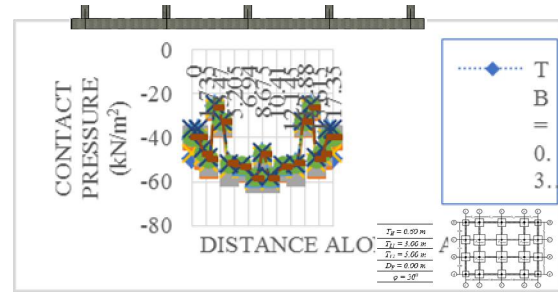


Figure [35] Comparison between contact pressure along axis (A-A) in case of static and dynamic load with different tie beam breadth where; $T_H = 0.60$ m, $T_{L1} = 3.00$ m, $T_{L2} = 5.00$ m, $D_F = 0.00$ and $\phi = 30^\circ$

Figure (35) show comparison between contact pressure in case of static load and dynamic load at different tie beam breadth where; $D_F = 0.00$ m, $\phi = 30^\circ$, $T_H = 0.60$ m, $T_{L1} = 3.00$ m, $T_{L2} = 5.00$ m.

Figures (36) and (37) show relationship between vertical shear stress and distance along axis (A-A) where; $D_F = 0.00$ m, $\phi = 30^\circ$, $T_H = 0.60$ m, $T_{L1} = 3.00$ m, $T_{L2} = 5.00$ m and different tie beam breadth in case of static and dynamic load respectively. From this figure; it can be shown the vertical displacement decreases by increasing tie beam breadth about (15) % in case of static load and dynamic load.

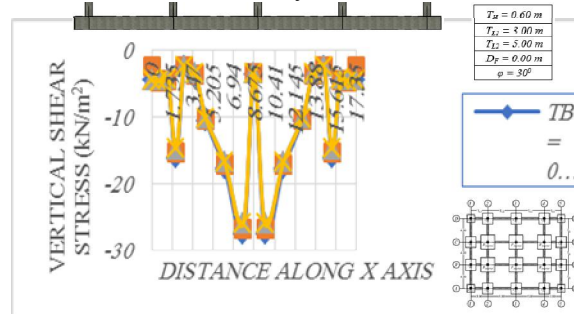


Figure [36] Relationship between vertical shear stress and distance along axis (A-A) in case of static load with different tie beam breadth where; $T_H = 0.60$ m, $T_{L1} = 3.00$ m, $T_{L2} = 5.00$ m, $D_F = 0.00$ and $\phi = 30^\circ$

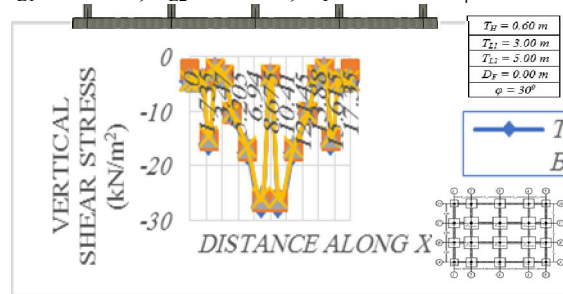


Figure [37] Relationship between vertical shear stress and distance along axis (A-A) in case of dynamic load with different tie beam breadth where; $T_H = 0.60$ m, $T_{L1} = 3.00$ m, $T_{L2} = 5.00$ m, $D_F = 0.00$ and $\phi = 30^\circ$

Figure (38) show comparison between vertical shear stress in case of static load and dynamic load at different tie beam breadth where; $D_F = 0.00$ m, $\phi = 30^\circ$, $T_H = 0.60$ m, $T_{L1} = 3.00$ m, $T_{L2} = 5.00$ m.



Figure [38] Comparison between vertical shear stress along axis (A-A) in case of static and dynamic load with different tie beam breadth where; $T_H = 0.60$ m, $T_{L1} = 3.00$ m, $T_{L2} = 5.00$ m, $D_F = 0.00$ and $\phi = 30^\circ$

Figures (39) and (40) show relationship between bending moment and distance along axis (A-A) where; $D_F = 0.00$ m, $\phi = 30^\circ$, $T_H = 0.60$ m, $T_{L1} = 3.00$ m, $T_{L2} = 5.00$ m and different tie beam breadth in case of static and dynamic load respectively. From this figure; it can be shown the vertical displacement decreases by increasing tie beam breadth about (30) % in case of static load and about (20) % in case of dynamic load.

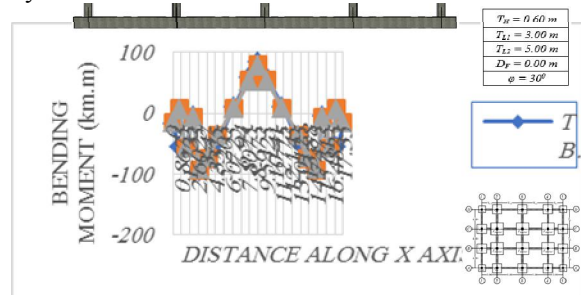


Figure [39] Relationship between bending moment and distance along axis (A-A) in case of static load with different tie beam breadth where; $T_H = 0.60$ m, $T_{L1} = 3.00$ m, $T_{L2} = 5.00$ m, $D_F = 0.00$ and $\phi = 30^\circ$

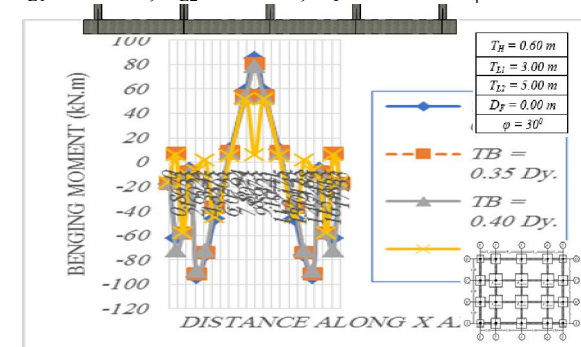


Figure [40] Relationship between bending moment and distance along axis (A-A) in case of dynamic load with different tie beam breadth where; $T_H = 0.60$ m, $T_{L1} = 3.00$ m, $T_{L2} = 5.00$ m, $D_F = 0.00$ and $\phi = 30^\circ$

Figure (41) show comparison between bending moment in case of static load and dynamic load at different tie beam breadth where; $D_F = 0.00$ m, $\phi = 30^\circ$, $T_H = 0.60$ m, $T_{L1} = 3.00$ m, $T_{L2} = 5.00$ m.

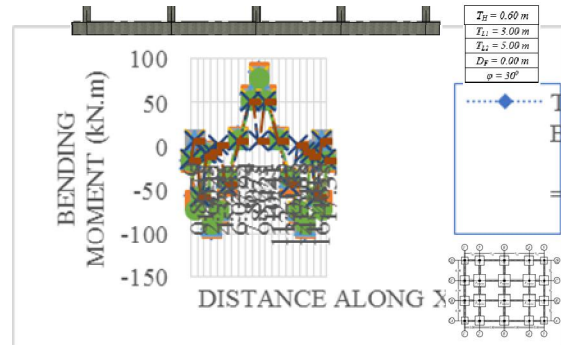


Figure [41] Relationship between bending moment and distance along axis (A-A) in case of dynamic load with different tie beam breadth where; $T_H = 0.60$ m, $T_{L1} = 3.00$ m, $T_{L2} = 5.00$ m, $D_F = 0.00$ and $\phi = 30^\circ$

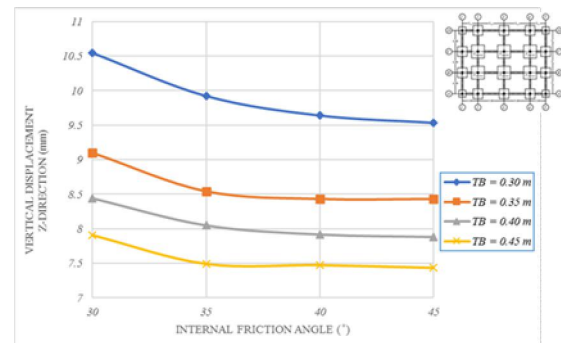


Figure [42] Relationship between maximum value of vertical displacement in Z-direction along axis (A-A) and internal friction angle in case of static load with different tie beam breadth where; $T_H = 0.60$ m, $T_{L1} = 3.00$ m, $T_{L2} = 5.00$ m and $D_F = 0.00$

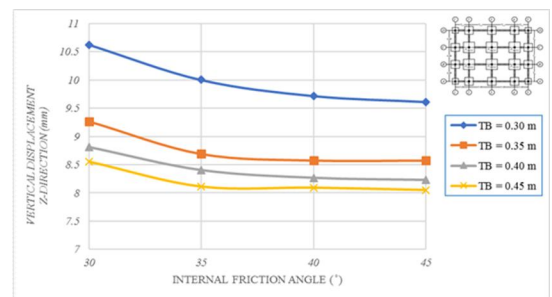


Figure [43] Relationship between maximum value of vertical displacement in Z-direction along axis (A-A) and internal friction angle in case of dynamic load with different tie beam breadth where; $T_H = 0.60$ m, $T_{L1} = 3.00$ m, $T_{L2} = 5.00$ m and $D_F = 0.00$

Figures (8-42) and (43) show the relationship between the value of maximum vertical displacement

in Z-direction under axis (A-A) and the internal friction angle (ϕ) where; $T_{L1} = 3.00\text{m}$ and $T_{L2} = 5.00\text{m}$ and $T_H = 0.60\text{m}$ as well as $D_F = 0.00\text{m}$ at different tie beam breadth in case of static and dynamic load respectively.

Figure (44) comparison between the value of maximum vertical in Z-direction in case of static load and dynamic load at different tie beam breadth where; depth of footing ($D_F = 0.00\text{ m}$), internal friction angle ($\phi = 30^\circ$), tie beam height ($T_H = 0.60\text{ m}$), tie beam length ($T_{L1} = 3.00\text{ m}$, $T_{L2} = 5.00\text{ m}$) and different tie beam breadth.

From these figures; it can be shown the vertical displacement in Z-direction decreases with increasing the internal friction angle for sandy soil up to $\phi \leq 36^\circ$ and in cases of $\phi > 36^\circ$ no significant change in the vertical displacement in Z-direction.

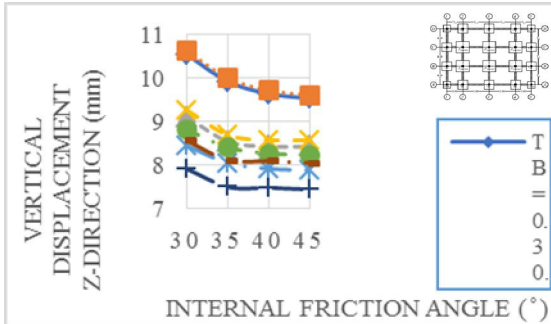


Figure [44] Comparison between maximum value of vertical displacement in Z-direction along axis (A-A) and internal friction angle in case of static load and dynamic load with different tie beam breadth where; $T_H = 0.60\text{ m}$, $T_{L1} = 3.00\text{ m}$, $T_{L2} = 5.00\text{ m}$ and $D_F = 0.00$

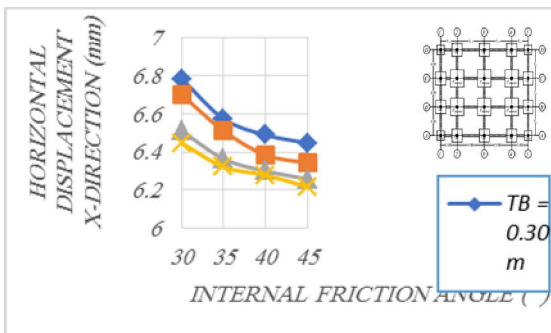


Figure [45] Relationship between maximum value of horizontal displacement in X-direction along axis (A-A) and internal friction angle in case of static load with different tie beam breadth where; $T_H = 0.60\text{ m}$, $T_{L1} = 3.00\text{ m}$, $T_{L2} = 5.00\text{ m}$ and $D_F = 0.00$

Figures (45) and (46) show the relationship between the value of maximum horizontal displacement in X-direction under axis (A-A) and the

internal friction angle (ϕ) where; $T_{L1} = 3.00\text{m}$ and $T_{L2} = 5.00\text{m}$ and $T_H = 0.60\text{m}$ as well as $D_F = 0.00\text{m}$ at different tie beam breadth in case of static and dynamic load respectively.

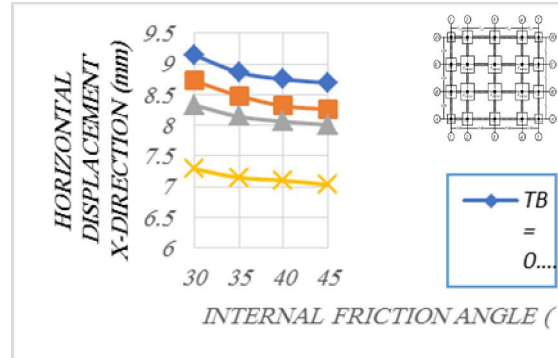


Figure [46] Relationship between maximum value of horizontal displacement in X-direction along axis (A-A) and internal friction angle in case of dynamic load with different tie beam breadth where; $T_H = 0.60\text{ m}$, $T_{L1} = 3.00\text{ m}$, $T_{L2} = 5.00\text{ m}$ and $D_F = 0.00$

Figure (47) comparison between the value of maximum horizontal in X-direction in case of static load and dynamic load at different tie beam breadth where; depth of footing ($D_F = 0.00\text{ m}$), internal friction angle ($\phi = 30^\circ$), tie beam height ($T_H = 0.60\text{ m}$), tie beam length ($T_{L1} = 3.00\text{ m}$, $T_{L2} = 5.00\text{ m}$) and different tie beam breadth.

From these figures; it can be shown the it can be shown the horizontal displacement in X-direction decreases with increasing the internal friction angle for sandy soil up to $\phi \leq 36^\circ$ and in cases of $\phi > 36^\circ$ no significant change in the vertical displacement in Z-direction.

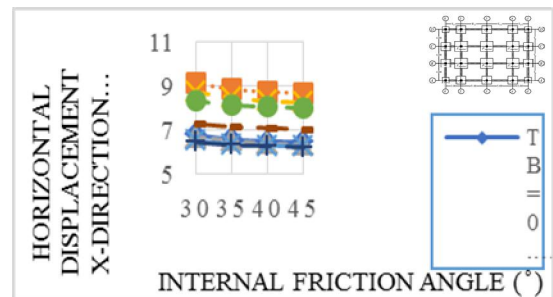


Figure [47] Comparison between maximum value of horizontal displacement in X-direction along axis (A-A) and internal friction angle in case of static load and dynamic load with different tie beam breadth where; $T_H = 0.60\text{ m}$, $T_{L1} = 3.00\text{ m}$, $T_{L2} = 5.00\text{ m}$ and $D_F = 0.00$

Figures (48) and (49) show the relationship between the value of maximum horizontal displacement in Y-direction under axis (A-A) and the

internal friction angle (ϕ) where; $T_{L1} = 3.00\text{m}$ and $T_{L2} = 5.00\text{m}$ and $T_H = 0.60\text{m}$ as well as $D_F = 0.00\text{m}$ at different tie beam breadth in case of static and dynamic load respectively.

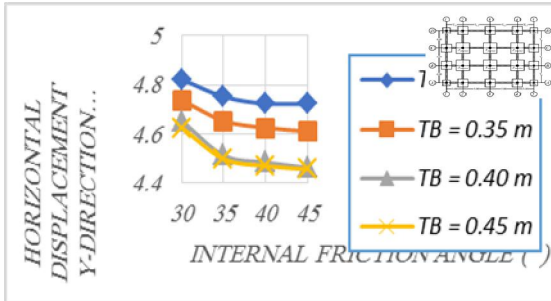


Figure [48] Relationship between maximum value of horizontal displacement in Y-direction along axis (A-A) and internal friction angle in case of static with different tie beam breadth where; $T_H = 0.60\text{ m}$, $T_{L1} = 3.00\text{ m}$, $T_{L2} = 5.00\text{ m}$ and $D_F = 0.00$

Figure (50) comparison between the value of maximum horizontal in Y-direction in case of static load and dynamic load at different tie beam breadth where; depth of footing ($D_F = 0.00\text{ m}$), internal friction angle ($\phi = 300$), tie beam height ($T_H = 0.60\text{ m}$), tie beam length ($T_{L1} = 3.00\text{ m}$, $T_{L2} = 5.00\text{ m}$) and different tie beam breadth.

From these figures; it can be shown the it can be shown the horizontal displacement in Y-direction decreases with increasing the internal friction angle for sandy soil up to $\phi \leq 36^\circ$ and in cases of $\phi > 36^\circ$ no significate change in the vertical displacement in Z-direction.

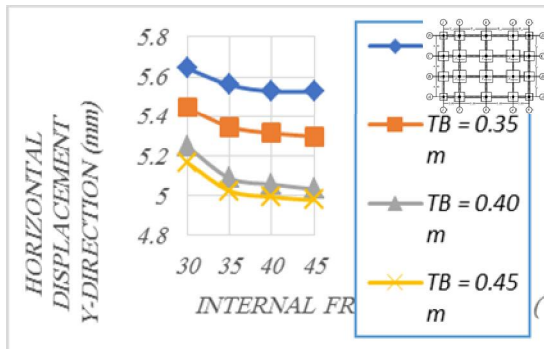


Figure (49) Relationship between maximum value of horizontal displacement in Y-direction along axis (A-A) and internal friction angle in case of dynamic load with different tie beam breadth where; $T_H = 0.60\text{ m}$, $T_{L1} = 3.00\text{ m}$, $T_{L2} = 5.00\text{ m}$ and $D_F = 0.00$

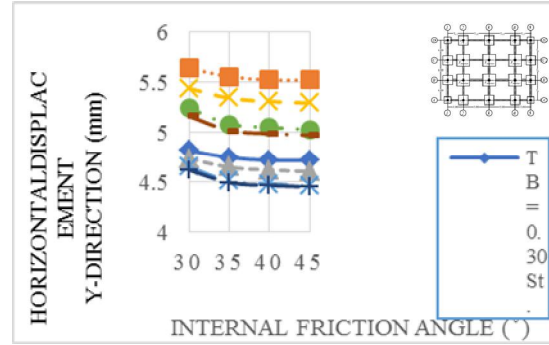


Figure [50] Comparison between maximum value of horizontal displacement in Y-direction along axis (A-A) and internal friction angle in case of static load and dynamic load with different tie beam breadth where; $T_H = 0.60\text{ m}$, $T_{L1} = 3.00\text{ m}$, $T_{L2} = 5.00\text{ m}$ and $D_F = 0.00$

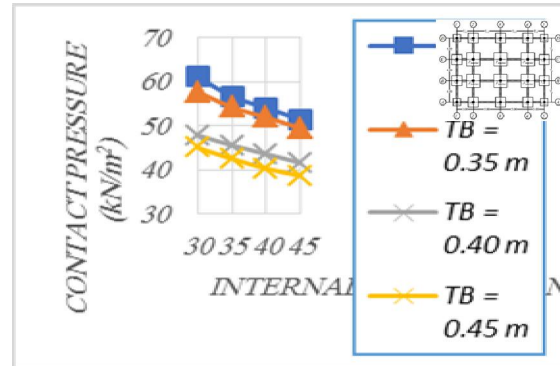


Figure [50] Relationship between maximum value of contact pressure along axis (A-A) and internal friction angle in case of static load with different tie beam breadth where; $T_H = 0.60\text{ m}$, $T_{L1} = 3.00\text{ m}$, $T_{L2} = 5.00\text{ m}$ and $D_F = 0.00$

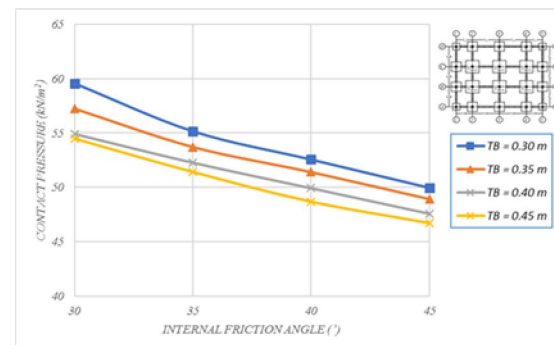


Figure [51] Relationship between maximum value of contact pressure along axis (A-A) and internal friction angle in case of dynamic load with different tie beam breadth where; $T_H = 0.60\text{ m}$, $T_{L1} = 3.00\text{ m}$, $T_{L2} = 5.00\text{ m}$ and $D_F = 0.00$

Figures (50) and (51) show the relationship between the value of maximum contact pressure under

axis (A-A) and the internal friction angle (ϕ) where; $T_{L1} = 3.00\text{m}$ and $T_{L2} = 5.00\text{m}$ and $T_H = 0.60\text{m}$ as well as $D_F = 0.00\text{m}$ at different tie beam breadth in case of static and dynamic load respectively.

Figure (52) comparison between the value of maximum contact pressure in case of static load and dynamic load at different tie beam breadth where; depth of footing ($D_F = 0.00\text{m}$), internal friction angle ($\phi = 30^\circ$), tie beam height ($T_H = 0.60\text{m}$), tie beam length ($T_{L1} = 3.00\text{m}$, $T_{L2} = 5.00\text{m}$) and different tie beam breadth.

From these figures; it can be shown that no significant change in total normal stress (contact pressure) distributions shape but the value of total normal stress decreases by increasing angle of internal friction. The value of total normal stress decreases by increasing tie beam breadth.

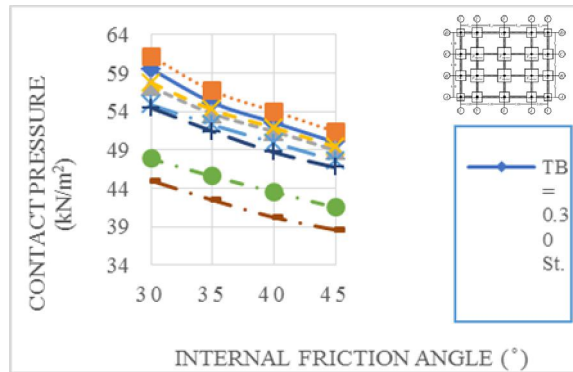


Figure [52] Comparison between maximum value of contact pressure along axis (A-A) and internal friction angle in case of static load and dynamic load with different tie beam breadth where; $T_H = 0.60\text{m}$, $T_{L1} = 3.00\text{m}$, $T_{L2} = 5.00\text{m}$ and $D_F = 0.00$

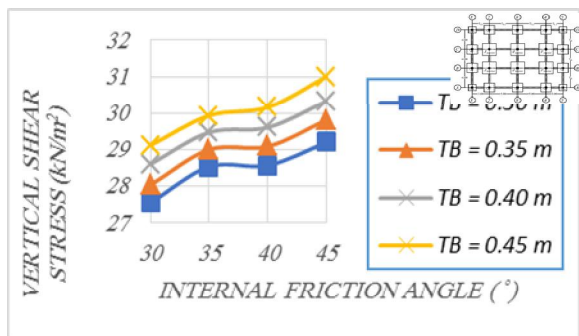


Figure [53] Relationship between maximum value of vertical shear stress along axis (A-A) and internal friction angle in case of static load with different tie beam breadth where; $T_H = 0.60\text{m}$, $T_{L1} = 3.00\text{m}$, $T_{L2} = 5.00\text{m}$ and $D_F = 0.00$

Figures (8-53) and (8-54) show the relationship between the value of maximum vertical shear stress under axis (A-A) and the internal friction angle (ϕ)

where; $T_{L1} = 3.00\text{m}$ and $T_{L2} = 5.00\text{m}$ and $T_H = 0.60\text{m}$ as well as $D_F = 0.00\text{m}$ at different tie beam breadth in case of static and dynamic load respectively.

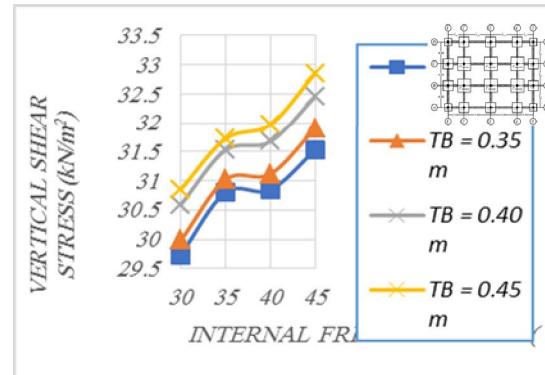


Figure [54] Relationship between maximum value of vertical shear stress along axis (A-A) and internal friction angle in case of dynamic load with different tie beam breadth where; $T_H = 0.60\text{m}$, $T_{L1} = 3.00\text{m}$, $T_{L2} = 5.00\text{m}$ and $D_F = 0.00$

Figure (55) comparison between the value of maximum vertical shear stress in case of static load and dynamic load at different tie beam breadth where; depth of footing ($D_F = 0.00\text{m}$), internal friction angle ($\phi = 30^\circ$), tie beam height ($T_H = 0.60\text{m}$), tie beam length ($T_{L1} = 3.00\text{m}$, $T_{L2} = 5.00\text{m}$) and different tie beam breadth.

From these figures; it can be shown that the value of vertical shear stress increases by increasing angle of internal friction.

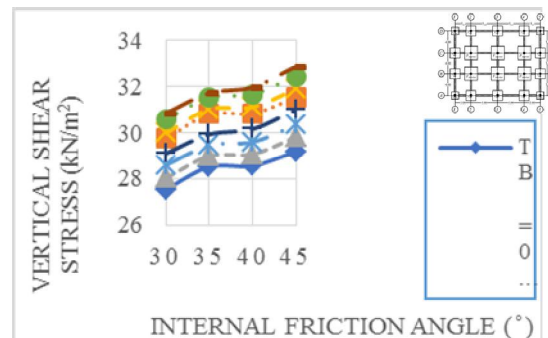


Figure [55] Comparison between maximum value of vertical shear stress along axis (A-A) and internal friction angle in case of static load and dynamic load at different tie beam breadth

Figures from (8-56) to (8-58) show the relationship between vertical displacement in Z direction and horizontal displacements in both X and Y directions and time at point (1) where; depth of footing ($D_F = 0.00\text{m}$), internal friction angle ($\phi = 30^\circ$), tie beam height ($T_H = 0.60\text{m}$), tie beam length

($T_{L1} = 3.00$ m, $T_{L2} = 5.00$ m) and different tie beam breadth in case of earthquake.

From these figures; it can be shown that the vertical displacement in Z-direction and horizontal displacements in both X and Y directions decreases with increasing tie beam breadth in case of dynamic load.

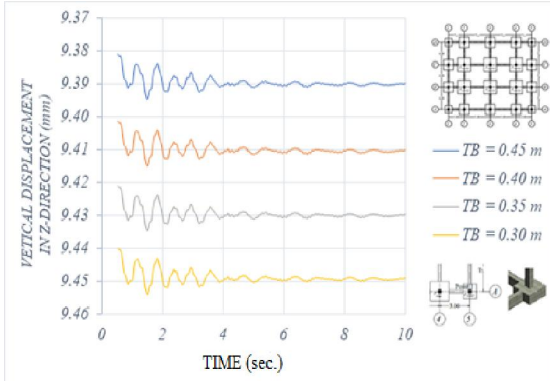


Figure [56] Relationship between vertical displacement in Z-direction and time at point (1) with different tie beam breadth with different tie beam breadth where; $T_H = 0.60$ m, $T_{L1} = 3.00$ m, $T_{L2} = 5.00$ m, $D_F = 0.00$ and $\phi = 30^\circ$

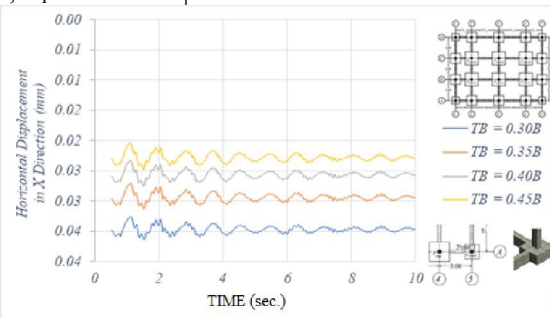


Figure [57] Relationship between horizontal displacement in X-direction and time at point (1) with different tie beam breadth with different tie beam breadth where; $T_H = 0.60$ m, $T_{L1} = 3.00$ m, $T_{L2} = 5.00$ m, $D_F = 0.00$ and $\phi = 30^\circ$

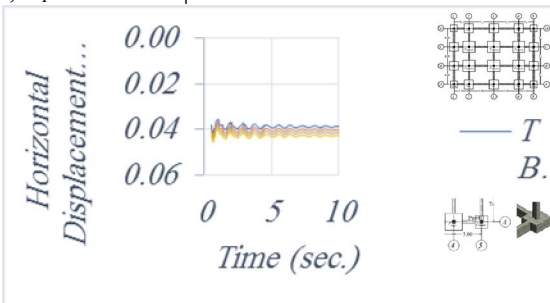


Figure [58] Relationship between horizontal displacement in Y-direction and time at point (1) with different tie beam breadth with different tie beam breadth where; $T_H = 0.60$ m, $T_{L1} = 3.00$ m, $T_{L2} = 5.00$ m, $D_F = 0.00$ and $\phi = 30^\circ$

5. Conclusions

From the present study the followings are concluded:

i. Increasing tie beam breadth leads to decreasing the vertical displacement in Z-direction about (10 to 25) % in case of static load as well as (10 to 20) % in case of dynamic load.

ii. Increasing tie beam breadth decreases the horizontal displacement in both X and Y directions about (30 to 50) % in case of static load as well as (15 to 30) % in case of dynamic load.

iii. By increasing tie beam breadth, the contact pressure decreases about (27) % in case of static load as well as (15) % in case of dynamic load.

iv. Increasing tie beam breadth leads to decreasing the vertical shear stress by (15) % in case of static load and dynamic load.

v. Increasing tie beam breadth decreases the bending moment about (30) % in case of static load as well as (20) % in case of dynamic load.

vi. The vertical displacement in Z-direction and horizontal displacement in both X and Y directions decreases with increasing the internal friction angle for sandy soil up to $\phi \leq 36^\circ$ and in cases of $\phi > 36^\circ$ no significant change in the vertical displacement in Z-direction and horizontal displacement in both X and Y directions.

vii. No significant change in contact pressure distributions shape but the value of total normal stress decreases by increasing angle of internal friction. The value of total normal stress decreases by increasing tie beam breadth.

viii. An inverse relationship between contact pressure and vertical shear stress as well as increasing internal friction angle increases the value of vertical shear stresses.

References

1. Almasmoum A.A. (2009) "influence of tie beams on the shallow isolated eccentric footing system" Journal of Engineering Sciences, Assiut University, Vol. 37, No. 1, pp.51 -61, January 2009.
2. Almasri, A.H. and Taqieddin, Z.N. (2012) Finite Element Study of Using Concrete Tie Beams to Reduce Differential Settlement Between Footings. Proceedings of the 13th WSEAS International Conference on Mathematical and Computational Methods in Science and Engineering, 112-116.
3. Al-Omari, R. R. and Al-Ebadi, L. H. (2008), "Effect of Tie Beams on Settlements and Moments of Footings" The 12th International Conference of International Association for Computer Methods and Advances in

- Geomechanics (IACMAG) October, Goa, India, PP. 3216 – 3223.
4. Basha, A.M. and Salama, M.I. (2017) "Finite Element Analysis of Tie Beams under the Effect of Differential Settlement of Isolated Footings" *Civil Engineering Journal* October 2017, 650-660.
 5. Elsamny, M.K., Abd Elsamee, W.N. and Elsedeeq M. B. (2010), "Effect of Depth of Foundation on Modulus of Elasticity "ES" For cohesionless Soil" *civil engineering research magazine*, Al-Azhar University.
 6. Elsamny, M. K., Abd Elsamee, W.N., Ezz-Eldeen, H.A. and Abo Al Anwar, M. (2012), "Settlement of Footings Connected with Tie Beam", *J. Of CERM*, Al Azhar University, Faculty of Engineering, Cairo, Egypt, Vol. 34 No. 2, January 2012, PP.
 7. El-Samny, M.K., Ezz-Eldeen, H.A., Elbatal, S.A. and Elsayed M.M. (2018) "Effect Of Eccentric Loading On Footings Connected With Tie Beams" *International Journal of Civil Engineering and Technology (IJCIET)* Volume 9, Issue 3, March 2018, pp. 200–220, Article ID: IJCIET_09_03_023.
 8. Elsamny, M. K., Ezz-Eldeen, H.A., Elbatal. S.A. and Kamar, A. M. (2017), "Effect of tie beam dimensions on vertical and horizontal displacement of isolated footing", *International Journal of Engineering Research & Technology*, Faculty of, Vol. 6 Issue 04, April-2017.
 9. Elsedeeq, M. B. (2013), "Effect of Overlap Stress as Well as Tie Beam Length and Width on Settlement of Isolated Footings Using Finite Element", *Open Journal of Civil Engineering*, 2014, 4, 35-44.
 10. Farouk, M. (2012), "Displacement Field of Shallow Foundation. Ph.D. Thesis, Faculty of Engineering, Al-Azhar University, Cairo.
 11. Khalil, A. A., (2000), "Soil Structure Interaction for Foundations Consisting of Isolated Footings and Connecting Walls or Beams" M.Sc. Thesis, *Structure Engineering Department*, Faculty of Engineering, Cairo University.
 12. Mahdy, M. (2011) *Settlement of Soil under Different Types of Foundations. Ph.D. Thesis*, Faculty of Engineering, Al-Azhar University, Cairo.
 13. Vincenzo Pane, Diego Bellavita, Giulio Castori, Alessia Vecchietti and Manuela Cecconi (2019), "On the interaction between spread foundations and tie-beams under eccentric loading" *Engineering Structures*, 109907, volume 204, 21 November 2019, doi: 10.1016/j.engstruct.2019.109907.

3/8/2020